Electronic Supplementary Material (ESI) for Dalton Transactions.

Electronic Supplementary Information

Pyrene based MOFs as fluorescent sensors for PAHs: an energetic pathway of backbone structure effect on response

Di Ning, Qiao Liu, Qian Wang, Xiao-Meng Du, Yue Li,* and Wen-Juan Ruan*

Synthesis of MOFs

NU-1000.[1] $ZrOCl_2 \cdot 8H_2O$ (97 mg, 0.3 mmol) and benzoic acid (2.7 g, 22 mmol) were dissolved in 8 mL of DMF via ultrasonication. The solution was placed in a vial and heated in an oven at 80 °C for 1 h. After cooling down to room temperature, H_4TBAPy (40 mg, 0.06 mmol) was added to it. The mixture was ultrasonicated for 20 min, and then heated at 80 °C for another 24 h. After cooling down, the yellow precipitate of NU-1000 was collected by centrifugation, washed with DMF (6×7 mL) and activated by HCl. To remove guest molecules, this material was finally soaked in methanol (5×10 mL) over 2 days and dried in vacuum at 60 °C for 6 h. Anal. Calcd. for $[Zr_6(\mu_3\text{-}O)_4(\mu_3\text{-}OH)_4(OH)_4(H_2O)_4(TBAPy)_2]$ (%): C, 48.51%; H, 2.02%; N, 0%. Found: C, 48.03%; H, 2.35%; N, 0 %.

NU-901.[2] 10 mL DMF solution containing $ZrOCl_2 \cdot 8H_2O$ (97 mg, 0.3 mmol) and *p*-aminobenzoic acid (1.5 g, 11 mmol) was heated at 80 °C for 1 h and then cooled to room temperature. After the addition of H_4TBAPy (40 mg, 0.06 mmol), the mixture was ultrasonicated for 20 min and subsequently heated at 100 °C for 12 h. After cooling down, the yellow powdered product was collected by centrifugation, washed with DMF (6×7 mL), and activated with HCl. The sample was soaked in methanol (5 × 10 mL) for 2 days to exchange guest molecules and dried in vacuum at 60 °C for 6 h. Anal. Calcd. for $[Zr_6(\mu_3\text{-}O)_4(\mu_3\text{-}OH)_4(OH)_4(H_2O)_4(TBAPy)_2]$ (%): C, 48.51%; H, 2.02%; N, 0%. Found: C, 47.23%; H, 2.96%; N, 0 %.

ROD-7.[3] $In(NO_3)_3 \cdot xH_2O$ (24 mg, 0.06 mmol) and H_4TBAPy (20 mg, 0.03 mmol) were dispersed in a mixed solvent of DMF (4 mL), dioxane (2 mL) and H_2O (2 mL), and 20 µL concentrated hydrochloric acid (6 M) was added to it. This mixture was ultrasonicated for 20 min and then heated at 85 °C for 24 h. After cooling down, the formed precipitate was collected by centrifugation, washed with DMF (6×7 mL), soaked in acetone (5×10 mL) for 2 days and dried in vacuum at 80 °C for 12 h. Anal. Calcd. for $[In_2(OH)_2(TBAPy)]$ (%): C, 56.03%; H, 2.54%; N, 0%. Found: C, 55.78%; H, 2.89%; N, 0 %.

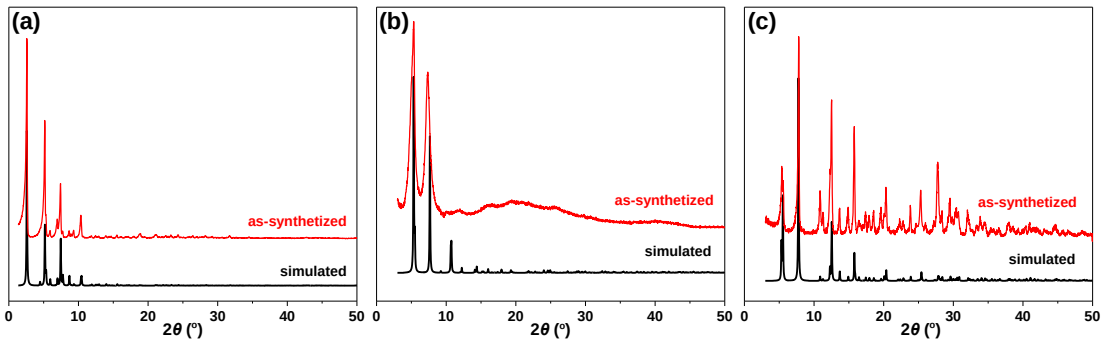

Fig. S1 PXRD patterns of as-synthesized (a) NU-1000, (b) NU-901 and (c) ROD-7 samples.

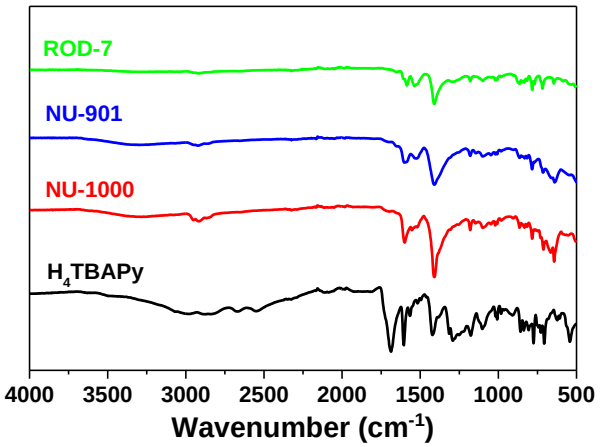

Fig. S2 FT-IR spectra of as-synthesized NU-1000, NU-901 and ROD-7 samples, the spectrum of free H_4TBAPy ligand is also provided for comparison. The carboxyl groups of H_4TBAPy ligands in NU-1000, NU-901 and ROD-7 give absorption peaks in the range of 1586~1603 cm^{-1}, which indicates that they are completely deprotonated during MOF formation.

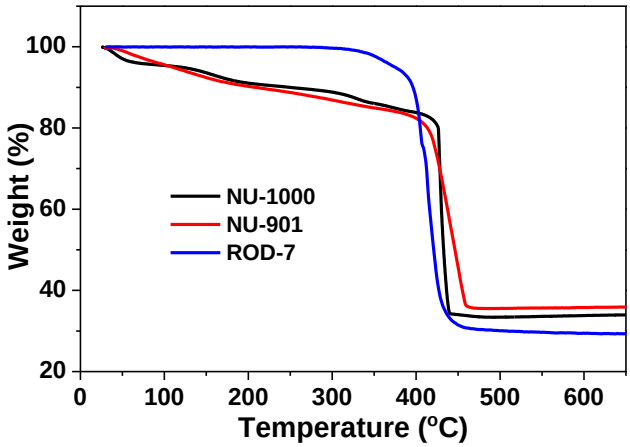

Fig. S3 Thermogravimetric curves of as-synthesized NU-1000, NU-901 and ROD-7 samples in airatmosphere. NU-1000 ($[Zr_6(\mu_3\text{-}O)_4(\mu_3\text{-}OH)_4(OH)_4(H_2O)_4(TBAPy)_2]$): The overall weight loss from room temperature to 650 °C is 66.11%, which could be assigned to the loss of all H_2O molecules, OH^- ions and organic components with ZrO_2 as residue (calcd. 66.03%). NU-901 ($[Zr_6(\mu_3\text{-}O)_4(\mu_3\text{-}OH)_4(OH)_4(H_2O)_4(TBAPy)_2]$): The overall weight loss is 64.47%, corresponding to the loss of all H_2O, OH^- and organic components (calcd. 66.03%). ROD-7 ($[In_2(OH)_2(TBAPy)]$): the first stage weight loss above 320 °C is due to the removal of OH^- and organic components (obsd. 70.46%, calcd. 70.54%).

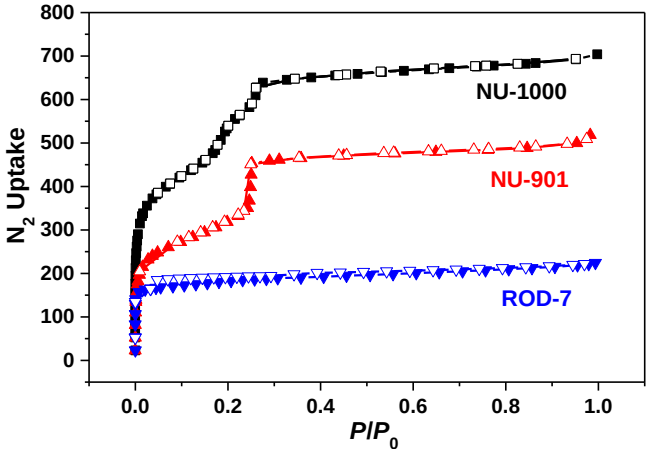

Fig. S4 N_2 adsorption isotherms (at 77 K) of activated NU-1000, NU-901 and ROD-7 samples.

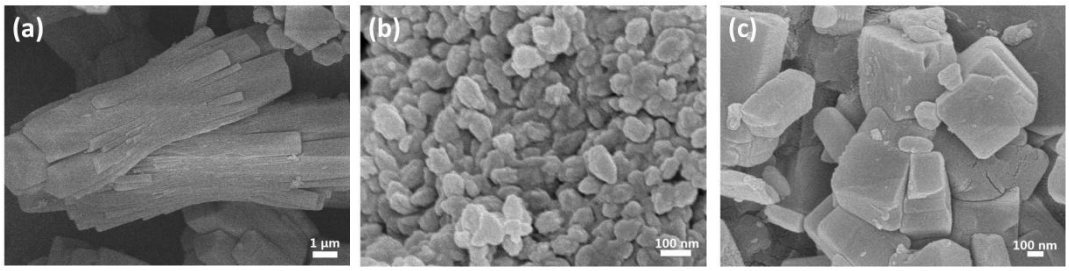

Fig. S5 SEM images of as-prepared (a) NU-1000, (b) NU-901 and (c) ROD-7 samples.

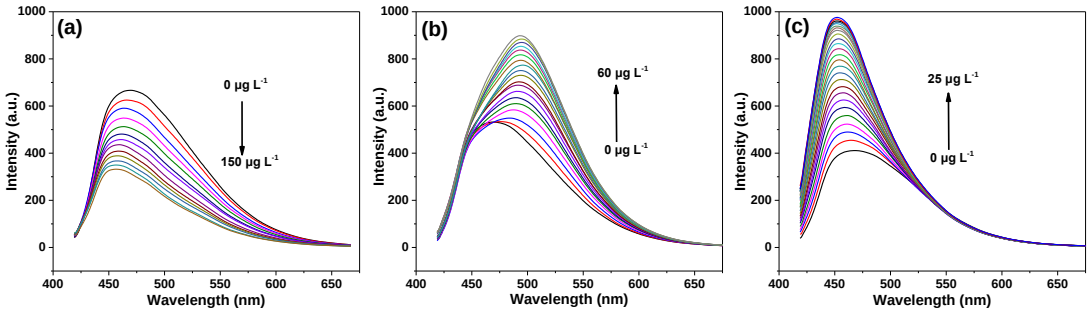

Fig. S6 Fluorescent spectra of the suspension of NU-1000 after the addition of different concentrations of (a) Acy, (b) Pyr and (c) Flt. The MOF concentration is 6.25 mg L^{-1} for (a) 5 mg L^{-1} for (b) and 3.75 mg L^{-1} for (c) to make the final fluorescent intensity in the measurement range, λ_{ex} = 395 nm.

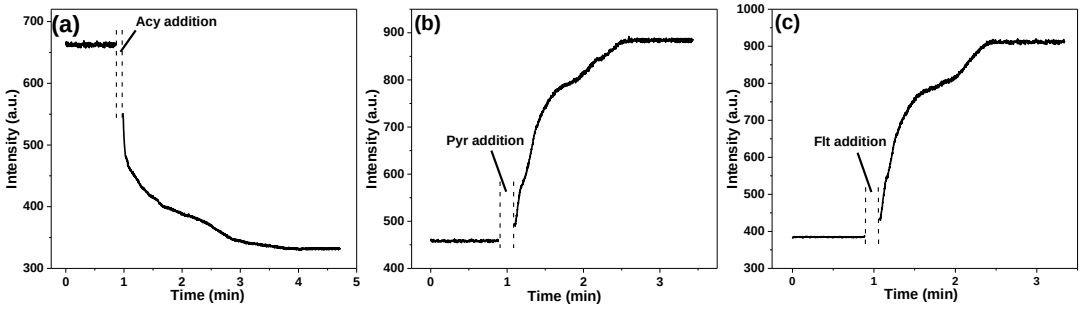

Fig. S7 Response time of NU-1000 to (a) Acy (150 μg L^{-1}), (b) Pyr (60 μg L^{-1}) and (c) Flt (25 μg L^{-1}). The concentration of NU-1000 is 6.25 mg L^{-1} for (a), 5 mg L^{-1} for (b) and 3.75 mg L^{-1} for (c), λ_{ex} = 395 nm.

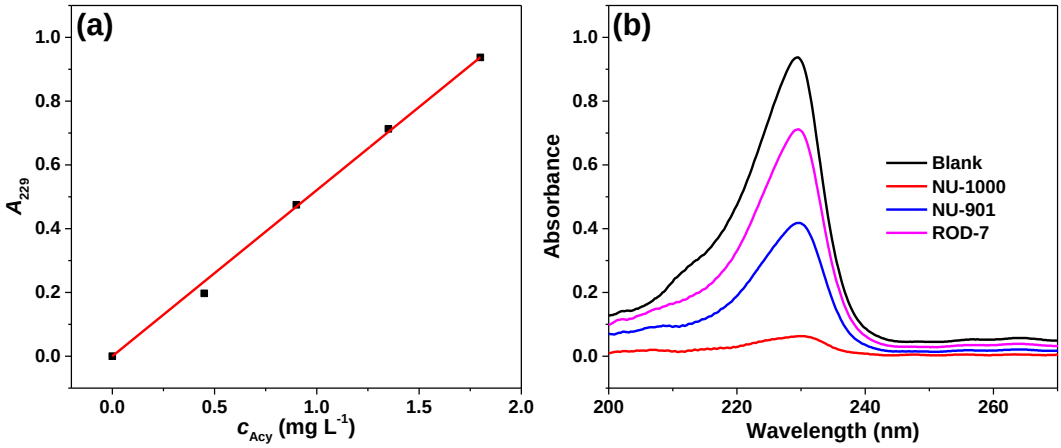

Fig. S8 (a) Calibration curve of the absorbance at 229 nm vs. Acy concentration in cyclohexane. (b) Absorption spectra of the extracts of Acy solution before and after the adsorption by NU-1000, NU-901 and ROD-7. 0.75 mg MOF was add to 150 mL aqueous solution of Acy (c_{Acy}^{0} = 60 μg L^{-1}) and stirred for 30 min. After the separation of MOF by centrifugation, the supernatant was extracted 3 times by 75 mL cyclohexane. The organic phase was combined, evaporated to 5 mL and subjected to UV-Vis measurement.

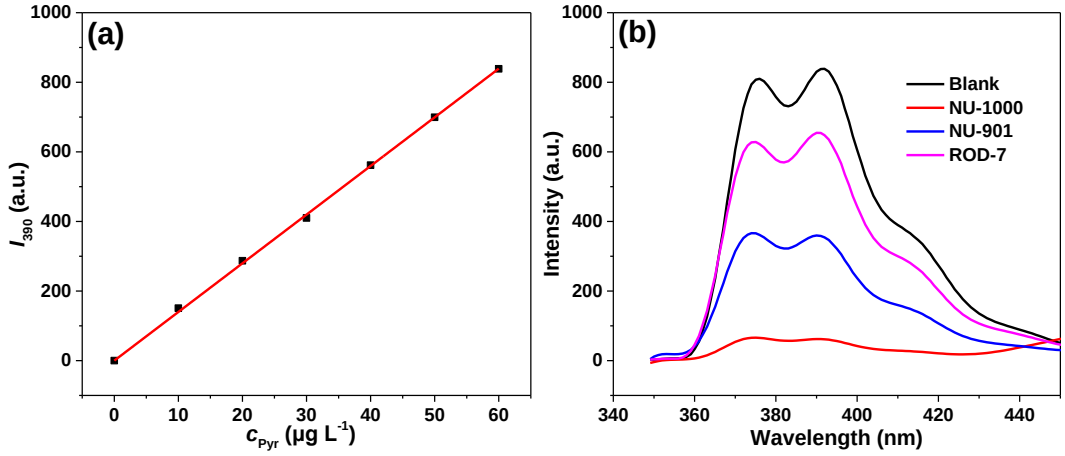

Fig. S9 (a) Calibration curve for the fluorescent quantification of Pyr at 390 nm. (b) Fluorescent spectra of Pyr solution (c_{Pyr}^{0} = 60 μg L^{-1}) before and after the adsorption by NU-1000, NU-901 and ROD-7. 15 μg MOF was add to 3 mL aqueous solution of Pyr and stirred for 30 min to establish adsorption−desorption equilibrium. After the separation of MOF by centrifugation, the fluorescent spectrum of the supernatant was measured with the excitation at 330 nm.

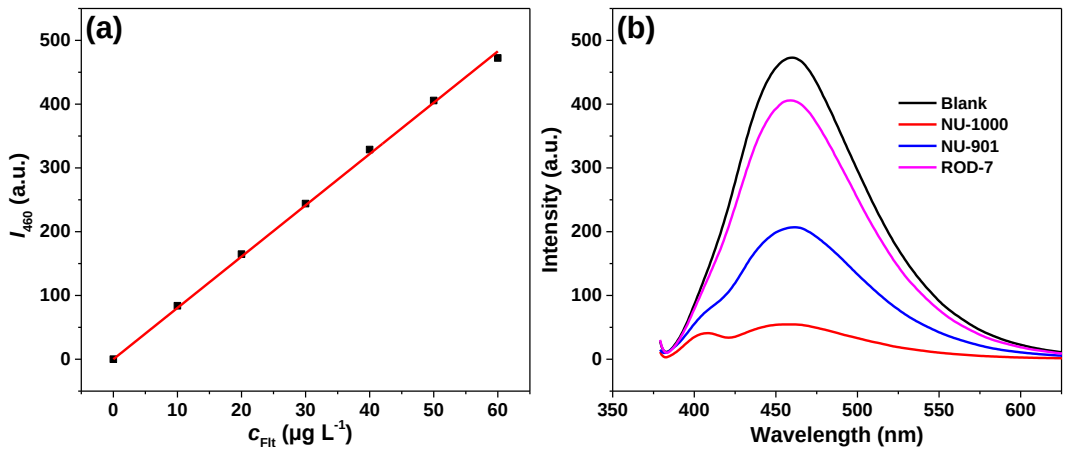

Fig. S10 (a) Calibration curve for the fluorescent quantification of Flt at 460 nm. (b) Fluorescent spectra of Flt solution (c_{Flt}^{0} = 60 μg L^{-1}) before and after the adsorption by NU-1000, NU-901 and ROD-7. 15 μg MOF was add to 3 mL aqueous solution of Flt and stirred for 30 min to establish adsorption−desorption equilibrium. After the separation of MOF by centrifugation, the fluorescent spectrum of the supernatant was measured with the excitation at 357 nm.

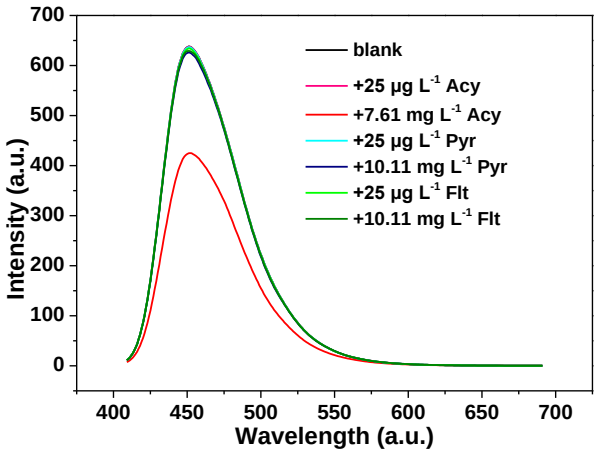

Fig. S11 Fluorescent spectra of the DMF solution of H_4TBAPy (4.69 μM) after the addition of Acy, Pyr, and Flt.

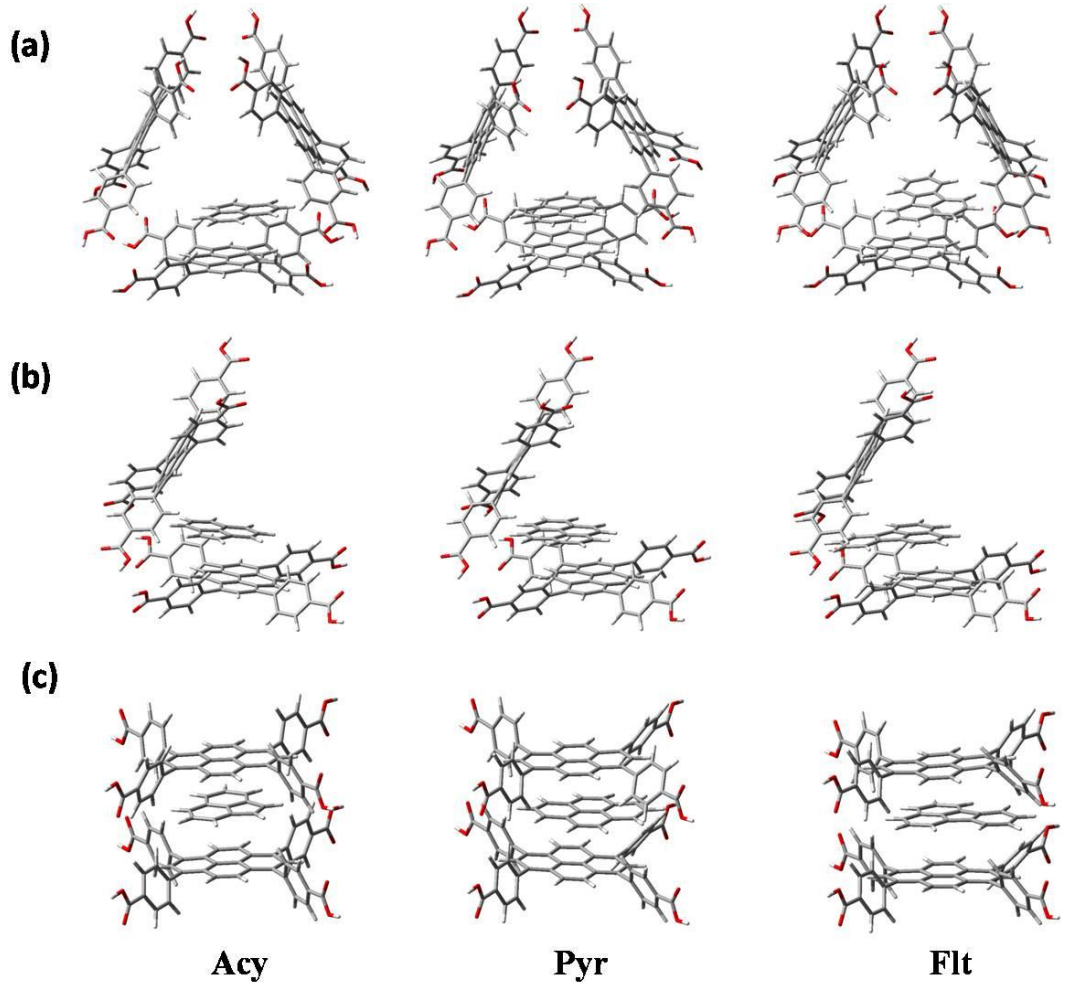

Fig. S12 Optimized adsorption configurations of Acy, Pyr and Flt on (a) NU-1000, (b) NU-901 and (c) ROD-7. Previous to the calculation about NU-1000, we have compared the binding energies of PAHs approaching from both the triangular and hexagonal pore sides. For all of Acy, Pyr and Flt, the adsorption in the triangular pore gives the more negative binding energy, so only these results are provided.

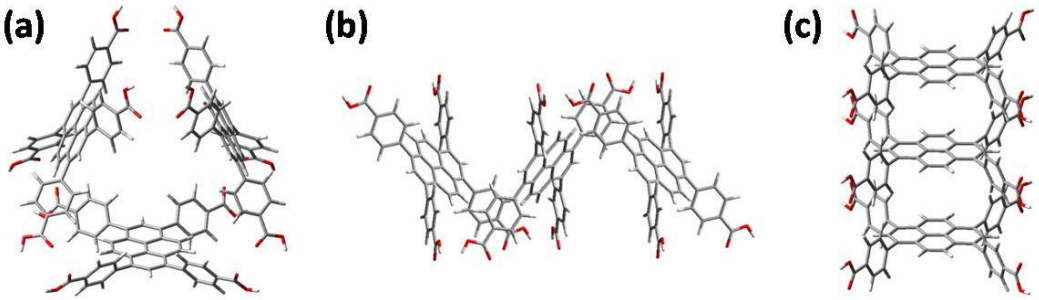

Fig. S13 The models used in the calculation about the oxidation potentials of (a) NU-1000, (b) NU-901 and (c) ROD-7.

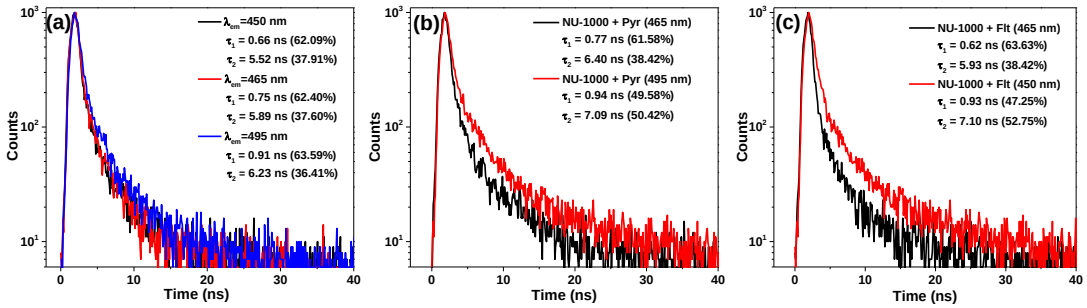

Fig. S14 Time-resolved fluorescent decays of NU-1000 in the presence of (a) none, (b) Pyr and (c) Flt. 5 mg L^{-1} NU-1000, 0.06 mg L^{-1} Pyr or Flt, λ_{ex} = 405 nm.

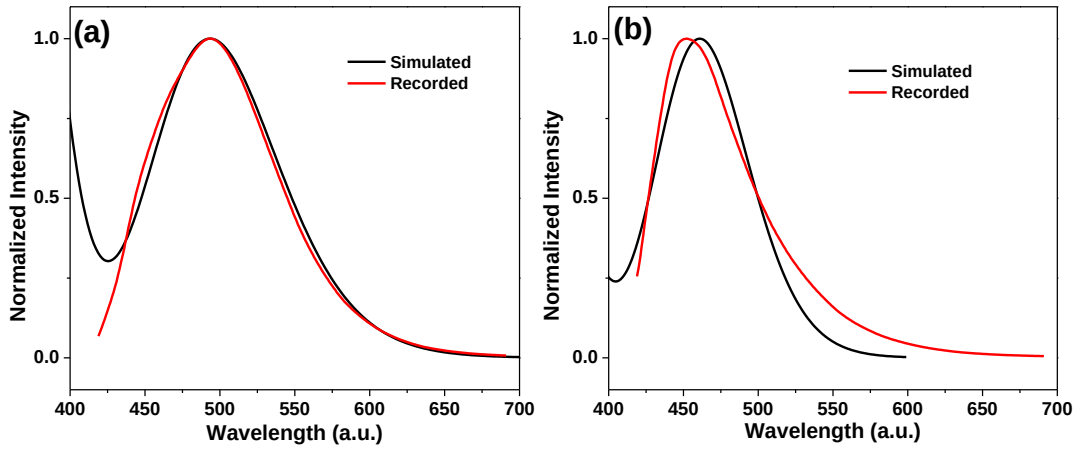

Fig. S15 Theoretically predicted and experimentally recorded emission spectra of (a) H_4TBAPy-Pyr excimer and (b) H_4TBAPy-Flt exciplex in the visible range.

Table S1 Binding energies of Acy, Pyr and Flt on MOFs

PAH	E_{PAHs} (hartree)	MOF	E_{MOF} (hartree)	$E_{complex}$ (hartree)	BSSE (hartree)	BE (kcal mol^{-1})
Acy	−461.9366	NU-1000	−6880.6737	−7342.6462	0.0076	−17.756
		NU-901	−4587.1177	−5049.0925	0.0090	−18.343
		ROD-7	−4587.0464	−5049.0412	0.0146	−27.316
Pyr	−615.5723	NU-1000	−6880.6737	−7496.2885	0.0087	−21.220
		NU-901	−4587.1177	−5202.7367	0.0108	−22.483
		ROD-7	−4587.0464	−5202.6739	0.0167	−24.128
Flt	−615.5505	NU-1000	−6880.6737	−7496.2681	0.0091	−21.783
		NU-901	−4587.1177	−5202.7193	0.0109	−25.185
		ROD-7	−4587.0464	−5202.6528	0.0170	−24.317

Table S2 Comparison between the calculated and measured reduction potentials of PAHs

PAH	$E_{molecule}$ (hartree)	E_{anion} (hartree)	$E(A^-/A)_{cal}$ (V vs NHE)	$E(A^-/A)_{exp}$ (V vs NHE)
Nap	−385.902	−385.974	−2.209	−2.296[b]
Acy	−462.106	−462.209	−1.358	−1.435[a]
Ace	−463.311	−463.375	−2.408	—[c]
Fln	−501.428	−501.493	−2.397	—[c]
Phe	−539.549	−539.623	−2.171	−2.247[b]
Ant	−539.542	−539.634	−1.639	−1.729[a]
Flt	−615.769	−615.867	−1.498	−1.566[a]
Pyr	−615.790	−615.877	−1.796	−1.830[a]
Baa	−693.192	−693.282	−1.706	−1.797[a]
Chr	−693.195	−693.276	−1.944	−2.002[a]

[a] Measured with cyclic voltammetry in anhydrous CH_3CN containing 0.1 M Bu_4NPF_6 as supporting electrolyte. The concentration of PAH was 120 mg L^{-1}. A gold electrode was used as working electrode at a scan rate of 50 mV S^{-1} (from −2.5 to 0 V), and the potentials were referenced to Ag/AgCl reference electrode and adjusted to reference vs. NHE. [b] From Ref. 4. [c] The reduction potentials of Ace and Flt are difficult to be measured because they are close to the edge of the potential window of CH_3CN, and no reported value could be found in literatures.

Table S3 Calculated reduction potentials of PAHs and oxidation potentials of MOFs

	E_{cation} (hartree)	$E_{molecule}$ (hartree)	E_{anion} (hartree)	$E(D/D^+)$ (V vs NHE)	$E(A^-/A)$ (V vs NHE)
Ligand	−2294.353	−2294.554	—	1.311	—
NU-1000	−6883.396	−6883.594	—	1.234	—
NU-901	−6883.261	−6883.460	—	1.273	—
ROD-7	−6883.297	−6883.499	—	1.342	—
Nap	—	−385.902	−385.975	—	−2.174
Acy	—	−462.107	−462.211	—	−1.324
Ace	—	−463.311	−463.376	—	−2.375
Fln	—	−501.428	−501.494	—	−2.365
Phe	—	−539.550	−539.624	—	−2.138
Ant	—	−539.542	−539.636	—	−1.607
Flt	—	−615.769	−615.868	—	−1.466
Pyr	—	−615.790	−615.878	—	−1.764
Baa	—	−693.192	−693.283	—	−1.676
Chr	—	−693.195	−693.278	—	−1.913

Table S4 Excited state binding energies and emission wavelengths of Pyr and Flt on MOFs.

PAH	E_{PAHs}^{ground} (hartree)	MOF	E_{ligand}^{exited} (hartree)	$E_{excimer/exciplex}$ (hartree)	Binding energy (kcal/mol)	λ_{em} (nm)
Pyr	−615.5723	NU-1000	−2293.4467	−2909.0643	−28.425	494
		NU-901	−2293.4456	−2909.0625	−27.966	485
		ROD-7	−2293.3883	−2909.0047	−27.667	474
Flt	−615.5505	NU-1000	−2293.4467	−2909.0398	−26.716	461
		NU-901	−2293.4456	−2909.0364	−25.229	456
		ROD-7	−2293.3883	−2908.9772	−24.075	433

References

1 D. Yang, S. O. Odoh, T. C. Wang, O. K. Farha, J. T. Hupp, C. J. Cramer, L. Gagliardi and B. C. Gates, *J. Am. Chem. Soc.*, 2015, **137**, 7391–7396.

2 M. H. Teplensky, M. Fantham, P. Li, T. C. Wang, J. P. Mehta, L. J. Young, P. Z. Moghadam, J. T. Hupp, O. K. Farha, C. F. Kaminski and D. Fairen-Jimenez, *J. Am. Chem. Soc.*, 2017, **139**, 7522–7532.

3 K. C. Stylianou, R. Heck, S. Y. Chong, J. Bacsa, J. T. A. Jones, Y. Z. Khimyak, D. Bradshaw and M. J. Rosseinsky, *J. Am. Chem. Soc.*, 2010, **132**, 4119–4130.

4 A. P. Davis and A. J. Fry, *J. Phys. Chem. C,* 2010, **114**, 12299–12304.